Accepted Manuscript

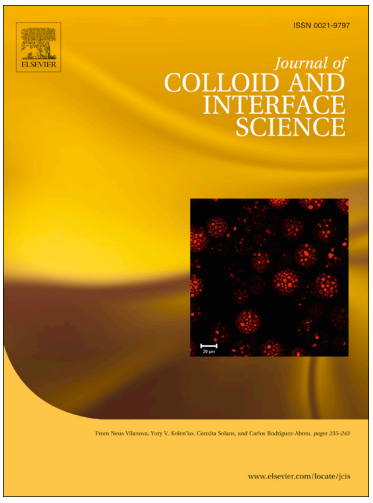

Bridging the Gap: Optimized Fabrication of Robust Titania Nanostructures on Complex Implant Geometries towards Clinical Translation

Tao Li, Karan Gulati, Na Wang, Zhenting Zhang, Sašo Ivanovski

PII: S0021-9797(18)30644-1
DOI: https://doi.org/10.1016/j.jcis.2018.06.004
Reference: YJCIS 23695

To appear in: *Journal of Colloid and Interface Science*

Received Date: 5 March 2018
Revised Date: 1 June 2018
Accepted Date: 3 June 2018

Please cite this article as: T. Li, K. Gulati, N. Wang, Z. Zhang, S. Ivanovski, *Bridging the Gap*: Optimized Fabrication of Robust Titania Nanostructures on Complex Implant Geometries towards Clinical Translation, *Journal of Colloid and Interface Science* (2018), doi: https://doi.org/10.1016/j.jcis.2018.06.004

Bridging the Gap: Optimized Fabrication of Robust Titania Nanostructures on Complex Implant Geometries towards Clinical Translation

Tao Li [a,b,c], Karan Gulati [a,b,d] ✉, Na Wang [c], Zhenting Zhang [c] and Sašo Ivanovski ✉ [a,b,d]

[a] School of Dentistry and Oral Health, Griffith University, Gold Coast, QLD, Australia

[b] Menzies Health Institute Queensland (MHIQ), Griffith University, Gold Coast, QLD, Australia

[c] Department of Prosthodontics, School of Stomatology, Capital Medical University, Beijing, People's Republic of China

[d] School of Dentistry, The University of Queensland, QLD, Australia

✉Corresponding Author

Prof. Sašo Ivanovski (s.ivanovski@uq.edu.au) and Dr. Karan Gulati (k.gulati@uq.edu.au)

School of Dentistry, University of Queensland, 288 Herston Road, Herston QLD 4006, Australia

Keywords: electrochemical anodization, titanium, nanopores, implants, mechanical stability

Abstract

Electrochemically anodized titanium surfaces with titania nanostructures (TNS; nanopores, nanotubes, etc.) have been widely applied as therapeutic bone/dental implant modifications. Despite the numerous advancements in the field of electrochemical anodization (EA), in terms of translation into the current implant market, the research gaps in this domain include the lack of fabrication optimizations performed on a substrate of conventional implant surface/geometry and inappropriate mechanical stability. In the current study, we investigate the role of substrate pre-treatment on achieving desired nanotopographies, reproducing optimized nanostructures on the complex geometry of commercial implant surfaces, and in-depth mechanical stability testing of these nano-engineered coatings. The results confirmed that: (a) Substrate polishing/smoothening may be insignificant with respect to fabrication of well-ordered and high quality TNS on micro-rough implants with preserved underlying micro-roughness. (b) Optimized outcomes can be successfully translated onto complex geometries characteristic of the current implant market, including dental implant abutments and screws (also applicable to a wider implant market including orthopaedics) (c) The mechanical stability testing revealed improved modulus and hardness values as compared to conventional nanotubes/pores. We believe that such optimization advances the existing knowledge of titanium anodization and anodized implants towards integration into the current implant market and successful clinical translation.

1. Introduction

Titanium is the ideal material choice for hard tissue fixation devices, such as orthopaedic and dental implants, due to its corrosion resistance and favourable biocompatibility [1]. In order to augment implant surface bioactivity and promote both early integration and long-term success, Ti surfaces have been modified at the macro, micro and nanoscales. Indeed, this represents one of the major research foci in the domain of orthopaedic/dental implants over the past few decades [2]. Extensive research has been performed towards tailoring the surface chemistry and topography of current Ti implants at the micro-scale, in order to enhance bone apposition at the implant interface [3]. However, since cellular function is mainly dictated by the interaction with the extracellular matrix on a nanoscale level, recent research focus has shifted towards enhancing surface bioactivity using nano-scale features [4,5]. Among the various nano-engineering techniques used for Ti surface modification, electrochemical anodization (EA) stands out due to its ability to facilitate fabrication of self-organized TiO_2 nanostructures (TNS, nanotubes or nanopores) via a simple, cost-effective and tailorable approach [6].

Numerous *in vitro* and *in vivo* studies have established that TNS are capable of promoting enhanced osseointegration and soft-tissue integration, as well as imparting antimicrobial and immunomodulatory properties, compared with conventional macro- or micro-rough Ti orthopaedic/dental implants [7-9]. Furthermore, the hollow architecture of the pores/tubes allows for the loading and local release of various therapeutics directly within the bone microenvironment, in order to target conditions such as infection, inflammation or poor integration [7-11]. Typically, the EA process on the titanium surface is carried out in aqueous/organic electrolyte containing fluoride ions and water, by applying a constant voltage or current to the electrochemical cell [12]. By optimizing electrolyte composition (ageing, water/fluoride content, pH) and anodization conditions (voltage, current, time), high quality and mechanically stable TNS can be fabricated with high-aspect ratio and tuneable dimensions [13,14].

In clinical dentistry, micro-roughness is regarded as the current ‘gold standard’ surface for achieving enhanced osseointegration, hence its preservation may be beneficial when further augmenting bioactivity through nanoscale modification [8]. Despite our ability to influence the EA process through various optimizations, it is still questionable whether pre-treatments of Ti surfaces (polishing and multi-step anodization)

play a role in improving the stability of TNS, especially on complex Ti surfaces characteristic of clinically utilized implants. Keeping all other parameters constant, in the current study, we focused on substrate preparation and its influence on the EA of micro-rough titanium, which represents a considerable portion of the commercial implant market.

Prior to EA, as-received titanium is often cleaned in order to remove surface-bound impurities. Furthermore, most EA is performed on smoothened Ti substrates, which enables improved ordering of TNS. Smoothening of the substrate is performed via chemical, mechanical and electro-polishing to remove surface artefacts, yielding a 'flat-bed' suitable for perpendicular growth of nanotubes/pores [15]. Although it has been shown that polishing results in mechanically stable anodic films, better ordering of tubes/pores and reduced surface defects, this does not necessarily apply for complex implant surface geometries [16]. In addition, nano-templated surfaces obtained by fabricating and removing the anodic film has gained much attention, which upon 2^{nd} EA yields highly ordered nanostructures [17-18]. Interestingly, both surface polishing and two-step EA (anodize, remove, re-anodize) are routinely practised for anodizing Ti (Fig. 1a), with applications ranging from therapeutic implants to solar cells and catalysis [13]. Indeed, the production of TNS for biological applications often involves polishing of the Ti substrate followed by a 2-step EA procedure, which can be detrimental towards preserving surface micro-roughness and overall costs (Fig. 1a).

For bone/dental implant applicability, the underlying implant substrate features are crucial for initial stability. However, the loss in active dimension due to polishing may compromise the initial implant fit and stability, which may lead to complete implant failure, especially in compromised conditions such as poor bone density [8]. Therefore, creating a dual topography with preserved existing micro-roughness and superimposed nanotubes/pores may be the ideal solution, as reported elsewhere [19]. Studies exploring such advanced hybrid structures often utilize multiple techniques (printing, patterning etc.) followed by EA [20]. However, for clinical translation, it would be highly relevant to fabricate such 'bioactive' nano-scale features superimposed on a preserved micro-roughness typical of existing commercially utilized implants.

Planar titanium foil, which represents the most commonly researched substrate choice for all applications involving biomedical titanium implants, represents an easy to manage surface. However, 'real world' commercially available implants are often curved with sharp edges (screws) and pins/wires/abutments (cylindrical), making

nanoscale surface modification via EA far more complex. Complex geometries increase the chance of anodic film cracks and delamination, owing to greater internal stresses, volume expansion and the presence of so-called 'weak spots' [21-23]. At the same time, reduced mechanical stability leading to fracture or delamination under handling, insertion or function, may compromise implant stability and lead to toxicity and complete failure [9,23]. Thus, studies aimed at optimizing the fabrication of mechanically robust TNS on complex Ti implant surfaces are critical for enabling the integration of nano-engineered implants from research into the current implant market.

In this study, we aim to address key research gaps related to the translation of anodized nano-engineered bone and dental implants into the commercial implant market, and hence clinical application. We start with as-received rough and mechanically prepared titanium substrate (reduced roughness/irregularity but still micro-rough), and perform single or two-step (anodize, remove and re-anodize) EA to fabricate various TNS, in an effort to investigate the role of surface polishing on the TNS yield. Key parameters were precisely monitored/controlled during each anodization, and the morphology and integrity of TNS layers was characterized by scanning electron microscopy (SEM). Later the optimized protocol was used to anodize Ti dental abutments (cylindrical) and screws, which represent commonly utilized implant geometries. Finally, in-depth assessment of the mechanical properties of the TNS, including elastic modulus and hardness, was carried out by nano-indentation testing. This study for the first time demonstrates the fabrication optimization of mechanically robust anodized nanostructures on commercial implant geometries/surfaces, thus reducing the gap between laboratory research and clinical implant industry.

2. Experimental

2.1 *Materials and chemicals*

Flat titanium foil ('Rough-Ti' 99.5% purity, 0.25 mm thick, 1 cm^2) and Ti wires (0.80 mm diameter, 99.5% purity) were purchased from Nilaco (Japan); pr-osteop (smooth) Ti screws (2.0 mm diameter and 3.0 mm length) were obtained from Southern Dental Implants (Irene, South Africa). Ethylene glycol (≥99 %) and ammonium fluoride (NH_4F, ≥99 %) were purchased from Sigma−Aldrich (Sydney, Australia).

2.2 *Ti surface pre-treatment*

Mechanical polishing was carried out on the 'Rough-Ti' foil with a gradient of sandpapers (500-1000 grit) in a unidirectional fashion ('Micro-Ti'). Prior to EA, Rough-Ti and Micro-Ti were cleaned by sonicating in acetone, ethanol and distilled water, and then dried in air.

2.3 *Two-step anodization*

TNS were fabricated via EA in a two-electrode electrochemical cell at room temperature using a DC power source (Keithley 2460, Ohio, USA) with the current precisely monitored. The Rough-Ti/Micro-Ti were used as anode and a titanium flat foil (5x5 mm, 0.25 mm thick) served as the counter electrode. In this study, we performed EA in a moisture-controlled system as previously described, with an ethylene glycol electrolyte containing 0.3 wt% NH_4F and 1 vol% deionized water [21]. Two different electrolyte systems were used for this study: fresh and aged. "Fresh electrolyte" represents the newly prepared electrolyte without any previous usage, whereas "aged electrolyte" represents pre-anodized electrolyte, which was repetitively anodized at 75V for 10 hours using non-target Ti [21,24]. To fabricate aligned nanopores, 1st EA was performed using aged electrolyte at 60V 10m. Alternatively, to enable easy removal of the anodic film, Rough-Ti and Micro-Ti were anodized at 75V for 2 hours using fresh electrolyte. The as-fabricated TNS layer was removed by ultra-sonication in methanol to obtain a nano-templated Ti surface (Rough-Template and Micro-Template) with nanotube-bottom imprints. Subsequently, the 2nd EA was performed using the textured Rough-Template and Micro-Template as the anode for 60V 10m in an aged electrolyte. Post fabrication, the samples were cleaned with deionized water and dried in air.

2.4 *Surface characterization of nano-engineered implants*

Surface topography of various substrates, templates and the fabricated TNS were investigated using Scanning electron microscope (SEM, Zeiss Sigma FESEM) by mounting the samples on a holder with double-sided conductive tape and coating with a 5nm thick platinum layer. A minimum of 3 samples were used for all characterizations.

2.5 *Anodization of dental implant surfaces*

Ti substrates representing commercial dental implants (abutments and screws) were anodized using the optimized EA conditions. For Ti wires (representative of dental abutments), the samples were thoroughly cleaned by sonicating in acetone, ethanol, and deionized water. The cleaned wires were masked using silicon tube, to expose a 5 mm length for anodization [23]. The screws (obtained as sterilized) and cleaned wires were

anodized at various voltages/times using appropriately aged electrolyte (10h aged). 1st EA, nanotemplate-fabrication (removal of anodic film) and 2nd EA were also performed on screws/wires as described in section 2.3. Post anodization, samples were cleaned using deionized water and dried in air for SEM characterization.

2.6 *Evaluation of mechanical properties*

Mechanical properties of the fabricated nanoporous structure on Ti abutment (wire) were evaluated by nanoindentation using a commercial nano-indenter [Hysitron TI 950 TriboIndenter]. The indentation was performed in the longitudinal direction of the nanopores at a maximum loading force of 10,000 μN with a Berkovich indenter (three-sided pyramid geometry), while the penetration depth of the tip was controlled to a maximum 10% of the total thickness of TNS film [25]. The anodized substrates were secured on the Al platform using superglue to avoid any movement during measurement. At least three indentations were performed on a single implant surface (total 3 implants were used), and elastic modulus and hardness values were obtained as a function of depth.

2.7 *Statistical analysis*

Data analysis was performed using SPSS 17.0 software (SPSS, Chicago, USA). One-way analysis of variance (ANOVA) followed by a post-hoc Bonferroni test was used to compare the data variation among different samples. $p < 0.05$ was considered to be significant. All experiments (fabrication, topographical characterization, current-time plots and mechanical testing) were performed in triplicate.

3. Results and Discussion

3.1 *Substrate Topography and Multi-Step Anodization*

The as-received titanium foil (Rough Ti) represents an extremely rough topography (Fig. 2A). Following mechanical treatment, the vertical rough features were reduced, yielding flattened yet anisotropic micro-features: Micro Ti (Fig. 2B). EA using aged electrolyte at 60V 10m yielded low-quality titania structures on Rough-Ti with visible surface defects (Fig. 2C), and ordered nanoporous architecture on Micro-Ti, with pores aligning along the direction of the underlying surface (Fig. 2D). Rough-Ti represents an extremely irregular surface topography and hence contains more ‘weak spots’, which when exposed to a very high local current density and growth rates, resulted in an irregular anodic film (without any

uniform nanopore formation/ordering) that is unsuitable for any applications [21]. On the contrary, EA of Micro-Ti resulted in aligned nanopores, whereby the pores followed the micro-scale features of the underlying substrate. Anodized Micro-Ti yielded crest and trough like dual micro-nano-structures as confirmed via SEM (Fig 2D) and AFM images (Fig S1, supporting information). The approximate dimensions of the nanopores (1st EA on Micro Ti) were ~50 nm diameter and ~8 µm length (please note that for Rough-Ti there was no uniformity with respect to porosity) . This feature is often achieved for single step EA, however, has never been explored towards any application. It is noteworthy that nanopores are more mechanically stable than conventional nanotubes, mainly because the individual tubes can bundle under stress and become prone to fracture [26]. More recently, we have shown that dual micro-rough and nanoporous titanium can enable increased proliferation and adhesion of osteoblasts and fibroblasts, while selectively reducing macrophage proliferation and attachment [27]. Moreover, fibroblasts and osteoblasts align in the direction of the aligned nanopores, as reported recently [27].

It is commonly accepted that the first anodic TiO_2 layer is poorly adherent to underlying substrates, and can be easily removed by ultra-sonication or mechanical bending [28]. On the contrary, for short duration EA in an aged electrolyte (60V 10m), 1st EA for Micro-Ti yielded stable anodic films. However, to enable easy removal of this fabricated anodic film, we anodized the substrates at 75V for 2hrs using fresh electrolyte (high water and active fluoride content) [21,29]. Upon detachment of this film, we could observe that the substrate was nano-templated (Fig. 2E-F). Clearly, a smoother and more porous topography of the titanium surface can be seen on the Micro-Ti nanotemplate (Micro-template, average diameter ~90 nm) (Fig 2F). On the contrary, Rough-template presented considerable disparity, with the entire surface patterned by random narrow pitting (Fig. 2E). Later, 2nd EA was performed on the nanotemplated substrates using 60V 10m (aged electrolyte) and the top-view SEM images are presented in Fig.2G-J. A well-adhered and crack-free porous layer was obtained for both surfaces, although the high-magnification insets (Fig. 2H,J) reveal a uniform structure on Micro-Ti. For 2nd EA a multi-pore structure is obtained, with pores grouped to form a larger pore but with a random arrangement, as presented in the insets Fig.2H,J. As reported previously, a hexagonal self-ordering can be obtained on a smooth surface by further removal and anodization cycles [17,30]. However, on the 2nd anodized Micro-Ti, without a surface smoothening step, nanopores with improved ordering was obtained (diameter of 'smaller' multi-pores ~ 42nm). This means that for a moderately

rough surface under controlled anodization conditions (electrolyte ageing), the 1st EA yields nanopores superimposed on micro-roughness (dual micro-nano), while the 2nd EA results in improved ordering of nanopores, thereby bypassing the need for a polished substrate. This reduces the overall steps involved towards nano-scale modification of micro-rough implants and at least partially preserves the underlying architecture. However, it is worth noting that the 2nd EA significantly reduces the micro-features of the underlying substrate.

Studies have reported that multi-step EA can significantly reduce surface roughness, as well as substrate defects such as grain boundaries and metallurgical defects, of the as-received Ti [31,32]. However, for biomedical applications including orthopedic and dental implants, it has been recognized that micro-roughness promotes initial implant stability and interlocking, and hence a superimposition of nanotopography (on existing micro-roughness) may be a better solution. Furthermore, substrate pre-treatment including polishing and multi-step anodization, can reduce the final active dimensions of the implant (at macro- and micro-scales), which can be detrimental to a secure fit at insertion (macro-features) and the rate and extent of osseointegration (micro-features). For example, in dentistry, a cavity slightly smaller than the diameter of the implant screw is drilled inside the bone to ensure good initial stability of the implant. The use of moderately rough Ti (Micro-Ti) and extremely irregular (Rough Ti) substrates thus represents a more clinically relevant implant topography compared to a very smooth surface, which is commonly used to demonstrate biomedical functionality of TNS. Furthermore, numerous studies have shown that two-step anodized TNS are hierarchical upper-porous/underneath-tubular structures [33,34]. The thin mesoporous top layer can effectively keep the underneath TNTs closely packed with surrounding tubes in parallel arrangement [17], and as a result the mechanical stability may be improved [26].

Furthermore, for EA using ethylene glycol based electrolytes, pre-utilization of electrolyte (ageing) enables improved ordering and stability of the anodic films [21]. To elucidate how a 1- or 2-step EA defines the structural integrity of the anodic film and the current profile for both fresh (unused) and aged electrolyte systems, we characterized the nanotopography (Fig. 3) and monitored the current-time plots (Fig. 4). A very interesting conclusion can be drawn with respect to 1st EA: for a fresh system (both for Rough- and Micro-Ti) a compromised and unstable anodic film displaying more cracks is observed, which can easily cause delamination (Fig. 3A-B). However, as shown above (Fig. 2C-D), using an aged electrolyte, 1st EA yielded much more adherent anodic films for both Rough

and Micro-Ti. Indeed, ageing the electrolyte enabled improved ordering of the nanopores for Micro-Ti, as compared to EA performed using fresh electrolyte. Furthermore, it is also evident that for Micro-Ti, 1st EA with fresh electrolyte did not yield improved alignment and/or preservation of the underlying topography. Interestingly, no significant differences in surface topography could be observed between the 2nd EA with fresh electrolyte system (Fig. 3C-F) and the aged system (Fig. 2G-J), for Rough- and Micro-Ti. Average pore diameter (multi-pore) for the fresh 2nd EA for Rough and Micro Ti were ~33 and ~29 nm, respectively.

The corresponding current-time plots comparing the aged and fresh systems for 1st and 2nd EA using both Rough and Micro-Ti substrates are presented in Fig. 4. For 1st EA, the aged system clearly showed high current values at all times, which corresponds to our previous findings [21]. Briefly, this can be attributed to the altered chemistry of the electrolyte, with reduced water and increased TiF_6 concentration (reduced electrical conductivity), thereby reducing both the oxide formation and oxide dissolution rates [21]. This delay in reaching the anodization equilibrium also results in the formation of a thicker barrier layer, which in turn enables stronger adherence to the substrate and a more compact and mechanically stable nanostructure film, mainly by alleviating the compressive stress at the oxide-metal interface [35]. However, for 2nd EA, it took less time to reach the anodization equilibrium phase (with a low and stable current value), as shown in Fig. 4C-D, and the current was always higher as compared with the corresponding times of the 1st EA (Fig. 4A-B). This can also be attributed to O_2 bubble formation and high current densities at the templated imprints left by the removal of 1st EA (nanotemplate) [36,37]. The reason for the high current values during the 2nd EA for Rough-Ti is the increased roughness/reduced ordering of the Rough-template as compared to the Micro-template (Fig. 2E-F).

To summarize, in the case of the fresh EA system, with the sufficient supply of water and active fluoride ions, high oxide formation and dissolution rates resulted in a similar current vs time behaviour between the substrates (Rough-Ti and Micro-Ti, and Rough-template and Micro-template) with the varied surface roughness, irrespective of whether a 1st and 2nd EA was used. However, in regards to the aged EA, the current corresponds to surface features such that for 1st EA: Micro-Ti reaches a plateau like stable current value (representative of equilibrium state) earlier as compared to the rougher counterpart (Rough-Ti). And for the aged- 2nd EA, no significant differences were observed with respect to time to reach the equilibrium state (as seen by reaching a stable current value). The high current

values (aged electrolyte) observed (Fig. 4D) for Rough-template can be attributed to the relatively higher number of surface irregularities compared to Micro-template, as seen in Fig. 2E,F. Higher surface roughness translates into increased number of 'weak spots' whereby very high local current densities can occur, as discussed previously [21].

3.2 *Fabrication of TiO_2 Nanostructures on Commercial Implants*

We extended the optimized anodization procedure as described above onto machined titanium wires (similar to dental abutments) and screws, which represent the commercial dental implant shape/geometry as shown in Fig. 5. The abutment (connector between the endosseous implant and the dental restoration) is cylindrical (Fig. 5A,C), while the implant screw has sharp edges at the threads, flat surface on the incline and the bottom curved surface (Fig. 5B,D). Furthermore all surfaces have 'machining' lines making the overall surface micro-rough in nature (Fig. 5C,D). The described 'grooved' dental implant micro-scale surfaces have been widely investigated and utilized in clinical practice over the past few decades [38].

The effects of anodization voltage (20-100V) on the quality of the nanoporous titania was investigated using a pre-conditioned electrolyte (10h aged) for 10 min. Fig. 6 shows the top-view SEM images of the anodized screw at the region of the screw-thread, whereby a very sharp edge (almost right angle) can create instability for the anodic film. It is worth noting that nanopores/tubes grow perpendicular to the substrate surface, and hence surface instabilities, cracks and delamination can easily occur at the acutely angled corner of the thread. The images of only 40-80V are presented in Fig. 6, because for EA<40V a non-porous oxide formation was formed, and >80V severely damaged/delaminated structures were obtained (Supporting Information, Fig. S2). From Fig. 6, it is evident that EA at 60V/10min creates the best conditions for preserved underlying substrate micro-features, with nanopores aligning on the substrate micro-machining lines and exhibiting comparatively few surface cracks and instabilities. On the contrary, 40V was not sufficient to enable fabrication of a porous architecture, while 80V, due to the high current and rapid growth rates, significantly compromised the integrity of the anodic film. Similar negative effects of higher growth rates induced by increased anodization voltage have also been recently reported on other substrate geometries, such as flat Ti foil and the curved wire [21,39]. It is established that higher anodization voltage increases the growth rate and hence the PBR (Pilling–Bedworth ratio: volume of oxide formed/metal consumed) during the anodic structure growth, which in turn can lead to poor adherence and compromised

mechanical stability. This effect is exacerbated for the very sharp thread of the Ti screw implant (as schematically represented in Fig. 7). From our results, it can be inferred that ageing of the electrolyte and the use of an appropriate anodization potential (60V) were effective towards fabricating robust anodic films on the complex screw surfaces. Using a previously optimized protocol, we also tried electropolishing of the Ti screws (data not presented) in order to smoothen the sharp edges, to prevent/reduce cracks on edges [21]. However, this approach has the inherent disadvantage of reducing the dimensions of the implant screw, which can cause complications for ensuring adequate fit and stability during surgical implantation.

In order to explore the potential for effective translation of EA to commercially relevant implant topographies and geometries, we anodized Ti wires (similar in shape to abutments) and Ti implant screws. Using the optimized fabrication protocol from the previous section, we were successful in achieving aligned nanopores, nanotemplate and random nanopores on both of these geometries. The surface topography of these structures, as characterized using SEM, is presented in Fig. 8. It is clear that the 1st EA preserved the underlying micro-scale features of these structures while superimposing nanotopography: dual micro-nano surface (Fig. 8A-D). Aligned nanoporous structures were reproduced onto the commercial implant geometries, with approximate porous diameters of ~45 nm and ~68 nm for wire and screw, respectively. These findings has two important implications; firstly, the need for substrate pre-treatment including polishing is eliminated (thus ensuring the dimensional stability of the implant), and the micro-roughness important for achieving osseointegration is preserved. It is worth noting that fabrication of nanotubes/nanopores on dental screw-shaped implants has been demonstrated previously, however, often using multi-step anodization procedures [38]. Having recently demonstrated that aligned nanopores allow for selective cellular bioactivity, these findings are significant towards fabrication optimization of such micro-nano architecture and clinical translation [27]. This also translates into having an abutment and a screw surface with abilities to promote soft-tissue integration and osseointegration respectively, while simultaneously achieving immuno-modulation [27]. Recently there have been attempts to modify bone implants to mimic the hierarchical structure of native bone, in an effort to enhance the rate and extent of implant osseo-integration. For instance, Zhao et al. reported a synergistic role of micro- and nano-topography towards achieving osteogenic responses with rat osteoblasts [40]. Furthermore, an *in vivo* study showed that hierarchical micro/nano-textured surfaces can

improve the osseointegration around Ti implants in ovariectomized sheep by further enhancing the osteogenic potential of micro-topography with superimposed nanoscale roughness [41].

Our optimized EA protocol enabled the fabrication of a hierarchical structure, consisting of a nanoporous coating superimposed on an underlying nanotubular architecture, as shown in the mechanically fractured anodic film in Fig. 8G. As reported elsewhere, these structures aid in shielding against any stresses encountered during handling or functioning, as the nanotubes are bound with the porous layer on top and hence are more mechanically robust than conventional nanotubes [26]. It is worth noting that no significant cracking or delamination was detected on the 2nd anodized abutment and screw surfaces, even at the sharp thread edges. The current–time transients recorded during the 2nd EA performed on the dental abutments and screws at 60V/10min are presented in Fig. S3 (Supporting Information).

Furthermore, nanotemplates (removal of 1st EA anodic film: Fig. 8E-G), and random nanopores (2nd EA on nanotemplates: Fig. 8H-J) can also be fabricated on commercial implant surfaces. Average template pore diameter for wire and screw as approximated from SEM images: 175 and 178 nm, respectively. It is interesting that nanotemplate-Ti has not been investigated for biomedical applications, since this titanium substrate consisting of the nano-prints of the delaminated nanotubes has the advantage of achieving controlled nanotopography without the risk of mechanical instability or delamination. Although nanotemplates are not suitable for drug release functions, they retain the mechanical characteristics of bulk titanium with nanopore/tube like topography. They can be used to distinguish between the effects of surface topography and chemistry, and hence can serve as a control when examining bioactivity of nanoporous or nanotubular implants. Additionally, we also fabricated stable random nanopores via 2nd EA as shown in Fig. 8H-J (average pore size of the multi-pores, wire 43 nm and screw 46 nm). Random multi-pores (pores within a pore) are generally fabricated on flat Ti, and have been reported to outperform conventional nanotubes in terms of photo-electrochemical characteristics due to their superior size uniformity and alignment [33]. Compared with the random nanopores achieved on a flat Ti foil (as presented in Fig. 2G-J), we have shown that high quality multi-pores can also be obtained on complex implant surfaces (Ti wire and screw) under the same anodization conditions. These results demonstrate the successful fabrication of various nanotopographies

on commercially relevant implant surfaces, which may promote further research into the clinical translation of nano-engineered therapeutic and bioactive implants.

3.3 *Comparison of Mechanical Characteristics*

Nano-indentation technique was utilized to quantify the mechanical properties of the TNS fabricated on the complex implant geometry. In this section, we focused on comparing the elastic modulus and hardness of titania nanopores fabricated using fresh and aged systems on the Ti wire (representative of a clinically relevant implant geometry) substrate (Table 1). Interestingly, such mechanical testing has only been restricted to planar foil substrates; however, since varied geometry can alter the integrity of the anodic film, it is crucial to study the mechanical properties of the complex anodized implant surfaces. The anodized Ti screw, with its varied surface features including narrow threads and sharp edges, did not allow for appropriate measurement of the mechanical characteristics, and hence the measurements were only performed on the Ti wire (abutment). Table 1 confirms that the elastic modulus of both structures increased with depth, but no significant difference observed for hardness values. This increase in elastic modulus may stem from the underlying Ti substrate effect and densification of the nanoporous structure during the test [26,42]. An important consideration is that a flat surface is generally preferred for nano-indentation assessment, rather than the complex nano-engineered implant geometries that are being investigated in this study. Therefore, we performed multiple measurements on several samples to obtain reliable and reproducible measurements of the mechanical robustness of anodized nanostructures superimposed on a more clinically relevant implant geometry [43]. The values presented in Table 1 are the mean values of several measurements (at least 3) performed on multiple samples (triplicate).

In terms of augmenting the mechanical stability of titania nanostructures on Ti surfaces, few studies have explored physical or chemical modification aimed at achieving the desirable mechanical properties: elastic modulus (23-44 GPa) and hardness (2.5 GPa) [44-46]. More recently, we have reviewed the key parameters influencing the mechanical properties of nanotubes and the various physio-chemical enhancements [26]. However, it is noteworthy that such nanotube modifications may alter the chemistry or topography of TNTs, which in turn can influence cell function. Herein, we propose the fabrication of dual micro-rough and nanoporous features on a complex implant geometry (Ti wire), which may

offer improved stability as compared to more commonly studied nanotubes fabricated on planar and smooth Ti substrates. In our study, the aligned TNPs fabricated by fresh and aged electrolyte systems exhibited a greatly enhanced elastic modulus (approximately 40-60GPa), which significantly outperformed conventional TNTs (4–8 GPa) [46]. The elastic modulus difference between the TNTs and TNPs can be explained by the fact that TNPs are compactly interconnected with surrounding pores, and such an arrangement enables sharing/distribution of the external compression forces [47]. This in turn can significantly reduce the strains on the anodic film that are encountered during implant handling, placement or function. It is worth noting that any delamination or fracture of the anodic film can initiate severe immunotoxicity responses and can lead to complete implant failure [9].

These mechanical enhancements, as demonstrated on Ti wire representative of geometries utilized in the wider implant market (meshes, pins, etc.), are achieved via an optimized single-step anodization, bypassing any polishing and/or multiple anodization steps (anodize, remove, re-anodize). Importantly, no physical or chemical treatments were performed (prior to, during or post EA) that may alter the surface topography or introduce new chemical groups, thereby avoiding the alteration of the established bioactivity and/or therapeutic function of the anodic nanostructures. Furthermore, as compared to the fresh-EA system, significantly enhanced stability of the dual micro-nanoporous structures was obtained with the aged system. This may be due to the improved preservation of the underlying micro-features for the aged EA, as demonstrated earlier [26]. Other reports have also shown that nanotopography superimposed on micro-patterned Ti can offer significantly enhanced adhesive strength between nanotubes and the underlying substrate [17]. It is also known that internal stress developed during EA growth due to volume expansion can also compromise the adhesive strength between anodic film and titanium substrate [48]. Therefore, increasing the interfacial area with micro-patterning methods can yield well-adhered and mechanically stable nanotubes/nanopores.

The current study aims at the effective utilization of various nanotopographies (aligned nanopores, nanotemplate, and random nanopores), which can be reproduced with minimal anodization steps while yielding stable/robust anodic nanostructures superimposed on the micro-roughness of complex implant geometries. When mechanical properties of TNPs were compared between fresh and aged electrolyte systems under the same time/voltage of anodization, the elastic modulus and hardness values confirmed a more robust nanoporous surface was obtained with the aged electrolyte (Table 1). A plausible explanation is that

preserved micro-grooves by electrolyte aging allowed for an extended interfacial contact area between the TNPs and the substrate, and as a result the mechanical stress and volume expansion during EA were reduced, which significantly enhanced TNPs mechanical stability [48,49]. More recently, Weszl et al. investigated the effects of EA parameters on the mechanical integrity and reproducibility of anodic TiO_2 nanotubes on the surface of dental implants (screws), and it was concluded that nanotubular titania modifications of commercial implant surfaces may have limited translational potential due to inadequate mechanical properties [50]. The formation of a fluoride-rich layer between the TNTs barrier layer and underlying substrate may also contribute towards the poor mechanical stability between the nanotubular film and the underlying substrate [26,51,52]. The chemical balance achieved during electrolyte ageing with limited water and active fluoride concentration translates into reduced chemical/fluoride attack, thereby augmenting mechanical stability of the anodic film (with preservation of underlying micro-roughness) which superimposes onto the micro-rough implant substrate [21]. To summarize, the fabrication optimization of mechanically robust titania nanopores superimposed onto the surface of clinically relevant micro-rough implant surfaces may aid in bridging the gap between nano-engineering based research and the current implant market and can promote the development of the next generation of therapeutic and bioactive titanium implants.

4. Conclusion

Titanium substrate polishing and 2-step anodization (anodize-remove-anodize) are considered essential towards fabrication of ordered nanotubular structures on titanium surfaces proposed for implant therapy applications [13-16]. These advancements have been demonstrated mostly for easy-to-manage planar Ti foils, but not on commercial implant geometries: wires, screws, meshes, etc. representing a wider orthopaedic/dental implant market [7]. Furthermore, substrate polishing and multi-step anodization results in removal of the underlying implant micro-roughness, which is considered crucial towards promoting osseointegration and initial stability [7]. In this study, we present a simple one-step anodization on micro-rough titanium (closely representing current implant topography) towards fabricating dual micro-rough and nanoporous implant surfaces. The resultant surface is presented with nanopores which are aligned in the direction of the underlying implant micro-machining lines. The surface pre-treatment steps are bypassed and the optimized results can be reproduced onto complex implant geometries, including dental

screws and abutments. Moreover, other nanotopographies including nanotemplates (removal of anodic film, titanium surface with no risk of mechanical failure) and random nanopores (2-step anodization) were also reproduced from planar Ti foil onto current implant geometries. Surface topography analysis, current-time transients and nanoindentation results were discussed in the context of optimizations performed on electrolyte chemistry (appropriately aged or fresh electrolyte), surface topography (rough, micro-rough or nano-templated) and number of anodization steps and voltage, with the aim to enable easy modification of titanium screws and wires/abutments. Furthermore, the nanopores, with preserved micro-roughness on complex surfaces via a single-step procedure, showed improved mechanical characteristics as compared to more commonly used nanotubes which are fabricated on polished planar titanium with multi-step anodization [26,45,46]. This study aids in bridging the gap between research and clinical implant industry, and advances the electrochemical anodization technique towards the fabrication of tailored nano-engineered titanium bone and dental implants.

Acknowledgements

Authors would like to thank the support from Central Analytical Research Facility (CARF) at Queensland University of Technology (QUT), Brisbane, Australia. KG is supported by the National Health and Medical Research Council (NHMRC) Early Career Fellowship (ECF), Peter Doherty-Australian Biomedical Fellowship (APP1140699).

References

[1] X. Liu, P.K. Chu, C. Ding, Surface modification of titanium, titanium alloys, and related materials for biomedical applications, Mater. Sci. Eng. R Rep. 47 (2004) 49-121.

[2] L. Le Guéhennec, A. Soueidan, P. Layrolle, Y. Amouriq, Surface treatments of titanium dental implants for rapid osseointegration, Dent. Mater. 23 (2007) 844-854.

[3] A.P. Tomsia, M.E. Launey, J.S. Lee, M.H. Mankani, U.G. Wegst, E. Saiz, Nanotechnology approaches for better dental implants, Int. J. Oral Maxillofac. Implants 26 (2011) 25.

[4] E.M. Christenson, K.S. Anseth, J.J. van den Beucken, C.K. Chan, B. Ercan, J.A. Jansen, C.T. Laurencin, W.J. Li, R. Murugan, L.S. Nair, Nanobiomaterial applications in orthopaedics, J. Orthop. Res. 25 (2007) 11-22.

[5] K.S. Brammer, C.J. Frandsen, S. Jin, TiO_2 nanotubes for bone regeneration, Trends Biotechnol. 30 (2012) 315-322.

[6] G.D. Sulka, J. Kapusta-Kołodziej, A. Brzózka, M. Jaskuła, Fabrication of nanoporous TiO_2 by electrochemical anodization, Electrochim. Acta 55 (2010) 4359-4367.

[7] K. Gulati, S. Maher, D.M. Findlay, D. Losic, Titania nanotubes for orchestrating osteogenesis at the bone–implant interface, Nanomedicine (Lond.) 11 (2016) 1847-1864.

[8] K. Gulati, S. Ivanovski, Dental implants modified with drug releasing titania nanotubes: therapeutic potential and developmental challenges, Expert Opin. Drug Deliv. 14 (2017) 1009-1024.

[9] K. Gulati, S. M. Hamlet, S. Ivanovski, Tailoring the Immuno-Responsiveness of Anodized Nano-Engineered Titanium Implants, J. Mater. Chem B 6 (2018) 2677-2689.

[10] C. Y. Cheng, H. Yang, Y. Yang, J. Huang, K. Wu, Z. Chen, X. Wang, C. Lin, Y. Lai. Progress in TiO2 nanotube coatings for biomedical applications: a review, J. Mater. Chem. B 6 (2018) 1862-1886.

[11] Q Wang, JY Huang, HQ Li, AZ Zhao, Y Wang, KQ Zhang, HT Sun, YK Lai, Recent advances on smart TiO2 nanotube platforms for sustainable drug delivery applications, Int. J. Nanomed. 12 (2017) 151-165.

[12] S. Kaneco, Y. Chen, P. Westerhoff, J.C. Crittenden, Fabrication of uniform size titanium oxide nanotubes: impact of current density and solution conditions, Scr. Mater. 56 (2007) 373-376.

[13] P. Roy, S. Berger, P. Schmuki, TiO_2 nanotubes: synthesis and applications, Angew. Chem. Int. Ed. 50 (2011) 2904-2939.

[14] K. Lee, A. Mazare, P. Schmuki, One-dimensional titanium dioxide nanomaterials: nanotubes, Chem. Rev. 114 (2014) 9385-9454.

[15] K. Lu, Z. Tian, J.A. Geldmeier, Polishing effect on anodic titania nanotube formation, Electrochim. Acta 56 (2011) 6014-6020.

[16] M. Fan, F. La Mantia, Effect of surface topography on the anodization of titanium, Electrochem. Commun. 37 (2013) 91-95.

[17] D. Wang, B. Yu, C. Wang, F. Zhou, W. Liu, A novel protocol toward perfect alignment of anodized TiO_2 nanotubes, Adv. Mater. 21 (2009) 1964-1967.

[18] J. Xing, L. Hui, Z. Xia, J. Chen, Y. Zhang, Z. Li, Influence of substrate morphology on the growth and properties of TiO_2 nanotubes in HBF_4-based electrolyte, Electrochim. Acta 134 (2014) 242-248.

[19] K. Gulati, M. Prideaux, M. Kogawa, L. Lima-Marques, G.J. Atkins, D.M. Findlay, D. Losic, Anodized 3D-printed titanium implants with dual micro- and nano-scale topography promote interaction with human osteoblasts and osteocyte-like cells, J. Tissue Eng. Regen. Med. 11 (2017) 3313-3325.

[20] D. Wang, T. Hu, L. Hu, B. Yu, Y. Xia, F. Zhou, W. Liu, Microstructured arrays of TiO_2 nanotubes for improved photo-electrocatalysis and mechanical stability, Adv. Funct. Mater. 19 (2009) 1930-1938.

[21] K. Gulati, A. Santos, D. Findlay, D. Losic, Optimizing anodization conditions for the growth of titania nanotubes on curved surfaces, J. Phys. Chem. C 119 (2015) 16033-16045.

[22] K. Gulati, M.S. Aw, D. Losic, Drug-eluting Ti wires with titania nanotube arrays for bone fixation and reduced bone infection, Nanoscale Res. Lett. 6 (2011) 571.

[23] K. Gulati, M. Kogawa, M. Prideaux, D.M. Findlay, G.J. Atkins, D. Losic, Drug-releasing nano-engineered titanium implants: therapeutic efficacy in 3D cell culture model, controlled release and stability, Mater. Sci. Eng. C 69 (2016) 831-840.

[24] H. Sopha, L. Hromadko, K. Nechvilova, J.M. Macak, Effect of electrolyte age and potential changes on the morphology of TiO_2 nanotubes, J. Electroanal. Chem. 759 (2015) 122-128.

[25] A.C. Fischer-Cripps, Contact mechanics, in: A.C. Fischer-Cripps, Nanoindentation, Springer New York, New York, 2011, pp. 1-19.

[26] T. Li, K. Gulati, N. Wang, Z. Zhang, S. Ivanovski, Understanding and Augmenting the Stability of Therapeutic Nanotubes on Anodized Titanium Implants, Mater. Sci. Eng. C, 88 (2018) 182-195.

[27] K. Gulati, H.J. Moon, T. Li, PT.S. Kumar, S. Ivanovski, Titania Nanopores with Dual Micro-/Nano-Topography for Selective Cellular Bioactivity, Mater. Sci. Eng. C, 2018 (in revision).

[28] J. Yan, F. Zhou, TiO_2 nanotubes: structure optimization for solar cells, J. Mater. Chem. 21 (2011) 9406-9418.

[29] D. Regonini, C. Bowen, A. Jaroenworaluck, R. Stevens, A review of growth mechanism, structure and crystallinity of anodized TiO_2 nanotubes, Mater. Sci. Eng. R Rep. 74 (2013) 377-406.

[30] G. Zhang, H. Huang, Y. Zhang, H.L. Chan, L. Zhou, Highly ordered nanoporous TiO_2 and its photocatalytic properties, Electrochem. Commun. 9 (2007) 2854-2858.

[31] J.Y. Choi, Y.H. Sung, H.J. Choi, Y.D. Kim, D. Huh, H. Lee, Fabrication of Au nanoparticle-decorated TiO_2 nanotube arrays for stable photoelectrochemical water splitting by two-step anodization, Ceram. Int. 43 (2017) 14063-14067.

[32] G. Ali, C. Chen, S.H. Yoo, J.M. Kum, S.O. Cho, Fabrication of complete titania nanoporous structures via electrochemical anodization of Ti, Nanoscale Res. Lett. 6 (2011) 332.

[33] F. Wang, Y. Liu, W. Dong, M. Shen, Z. Kang, Tuning TiO_2 photoelectrochemical properties by nanoring/nanotube combined structure, J. Phys. Chem. C 115 (2011) 14635-14640.

[34] Z. Zhang, P. Wang, Optimization of photoelectrochemical water splitting performance on hierarchical TiO_2 nanotube arrays, Energy Environ. Sci. 5 (2012) 6506-6512.

[35] X. Zhou, N.T. Nguyen, S. Özkan, P. Schmuki, Anodic TiO_2 nanotube layers: why does self-organized growth occur—a mini review, Electrochem. Commun. 46 (2014) 157-162.

[36] J. Oh, C.V. Thompson, The role of electric field in pore formation during aluminum anodization, Electrochim. Acta 56 (2011) 4044-4051.

[37] S. Yan, Y. Chen, Z. Wang, A. Han, Z. Shan, X. Yang, X. Zhu, Essential distinction between one-step anodization and two-step anodization of Ti, Mater. Res. Bull. 95 (2017) 444-450.

[38] I. Jang, S. Shim, D. Choi, B. Cha, J. Lee, B. Choe, W. Choi, Effect of TiO2 nanotubes arrays on osseointegration of orthodontic miniscrew, Biomed. Microdevices 17 (2015) 76.

[39] S.P. Albu, P. Schmuki, Influence of anodization parameters on the expansion factor of TiO_2 nanotubes, Electrochim. Acta 91 (2013) 90-95.

[40] L. Zhao, S. Mei, P.K. Chu, Y. Zhang, Z. Wu, The influence of hierarchical hybrid micro/nano-textured titanium surface with titania nanotubes on osteoblast functions, Biomaterials 31 (2010) 5072-5082.

[41] J. Xiao, H. Zhou, L. Zhao, Y. Sun, S. Guan, B. Liu, L. Kong, The effect of hierarchical micro/nanosurface titanium implant on osseointegration in ovariectomized sheep, Osteoporos. Int. 22 (2011)1907-1913.

[42] Y. Xu, M. Liu, M. Wang, A. Oloyede, J. Bell, C. Yan, Nanoindentation study of the mechanical behavior of TiO_2 nanotube arrays, J. Appl. Phys. 118 (2015) 145301.

[43] S. Bull, Nanoindentation of coatings, J. Phys. D 38 (2005) R393.

[44] T. Shokuhfar, G.K. Arumugam, P.A. Heiden, R.S. Yassar, C. Friedrich, Direct compressive measurements of individual titanium dioxide nanotubes, ACS Nano 3 (2009) 3098-3102.

[45] F. Schmidt-Stein, S. Thiemann, S. Berger, R. Hahn, P. Schmuki, Mechanical properties of anatase and semi-metallic TiO_2 nanotubes, Acta Mater. 58 (2010) 6317-6323.

[46] G. Crawford, N. Chawla, J. Houston, Nanomechanics of biocompatible TiO_2 nanotubes by interfacial force microscopy (IFM), J. Mech. Behav. Biomed. Mater. 2 (2009) 580-587.

[47] H. Hirakata, K. Ito, A. Yonezu, H. Tsuchiya, S. Fujimoto, K. Minoshima, Strength of self-organized TiO_2 nanotube arrays, Acta Mater. 58 (2010) 4956-4967.

[48] J. Proost, J.-F. Vanhumbeeck, Q. Van Overmeere, Instability of anodically formed TiO_2 layers (revisited), Electrochim. Acta 55 (2009) 350-357.

[49] N.B. Pilling, R.E. Bedworth, The oxidation of metals at high temperatures, J. Inst. Met. 29 (1923) 529−591.

[50] M. Weszl, K.L. Tóth, I. Kientzl, P. Nagy, D. Pammer, L. Pelyhe, N.E. Vrana, D. Scharnweber, C. Wolf-Brandstetter, Á. Joób, Investigation of the mechanical and

chemical characteristics of nanotubular and nano-pitted anodic films on grade 2 titanium dental implant materials, Mater. Sci. Eng. C 78 (2017) 69-78.

[51] H. Habazaki, K. Fushimi, K. Shimizu, P. Skeldon, G.E. Thompson, Fast migration of fluoride ions in growing anodic titanium oxide, Electrochem. Commun. 9 (2007) 1222-1227.

[52] K. Shimizu, K. Kobayashi, G.E. Thompson, P. Skeldon, G.C. Wood, Anodic oxide films on tantalum: incorporation and mobilities of electrolyte-derived species, Phil. Mag. B 73 (1996) 461.

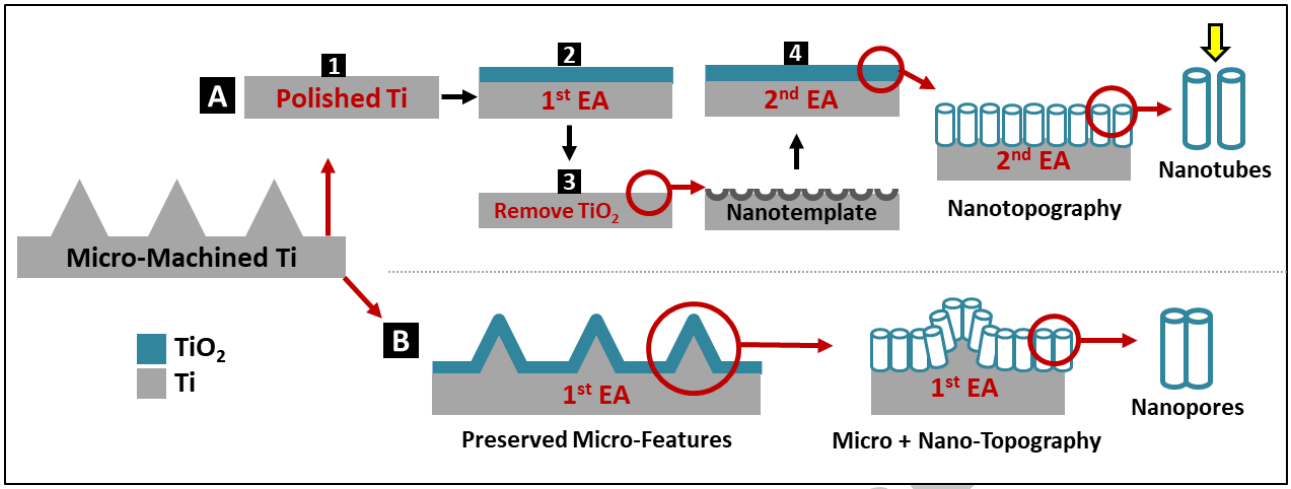

Fig. 1. Representation of the fabrication of nano-engineered Ti via electrochemical anodization (EA) on a micro-rough surface (images represent a cross-sectional view): (A) conventional protocol: (1) polishing, (2) 1st EA, (3) removal of anodic film-nanotemplate, and (4) 2nd EA, yielding nanotubes which are more prone to damage/delamination due to space between individual tubes (yellow arrow). (B) Preserving underlying substrate micro-features and superimposing nanopores, via single step EA (under optimum conditions), yielding a dual micro-and nano-scale topography.

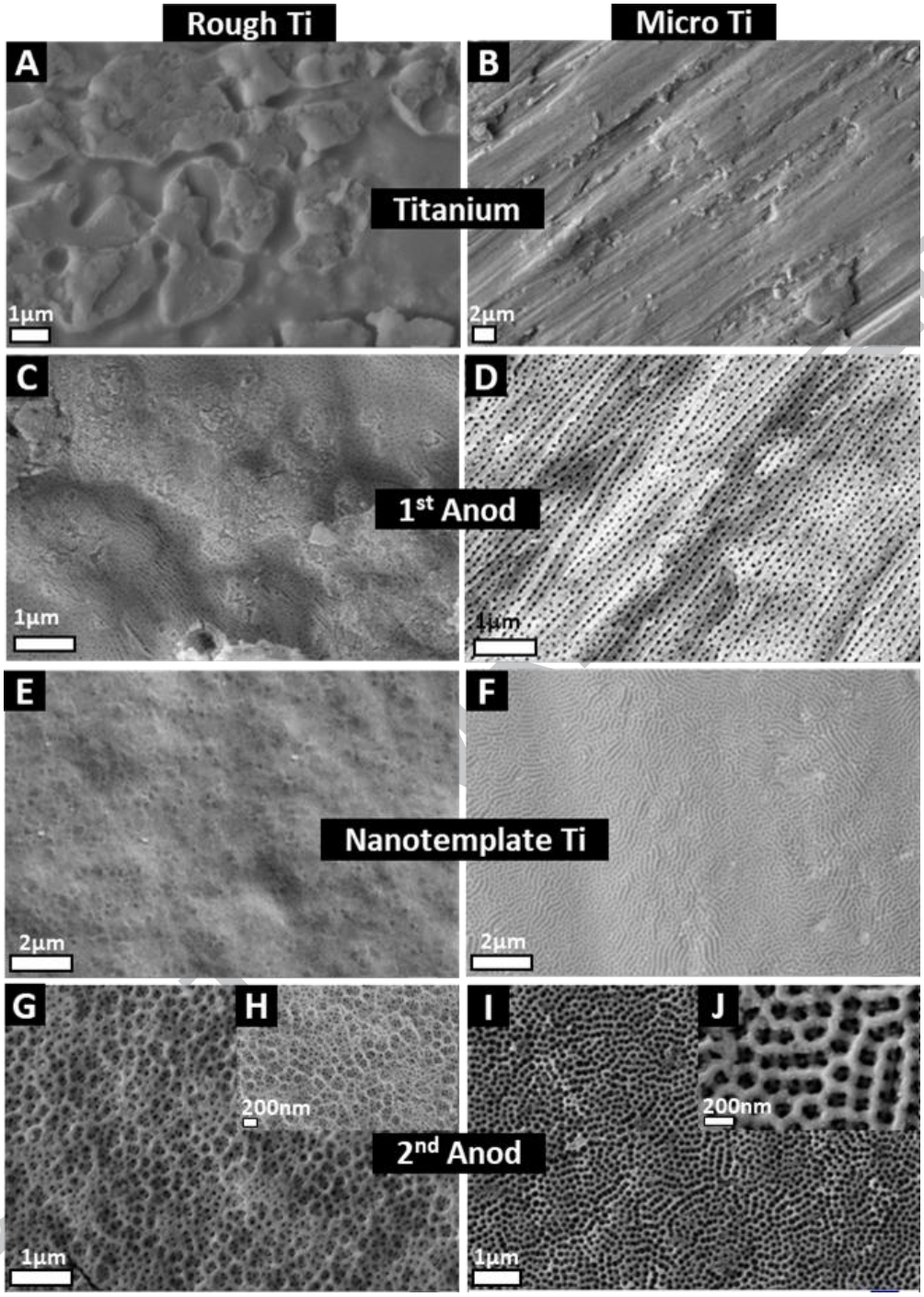

Fig. 2. Top-view SEM images: (A) as received Rough-Ti, (B) mechanically prepared Micro-Ti, (C-D) 1st anodized TNPs (aged EA system 60V 10min), (E-F) nano-templated surfaces (fresh electrolyte, 75V 2h, anodic layer removed), and (G-J) 2nd anodized TNPs (aged EA system 60V 10min). EA: electrochemical anodization; TNPs: titania nanopores.

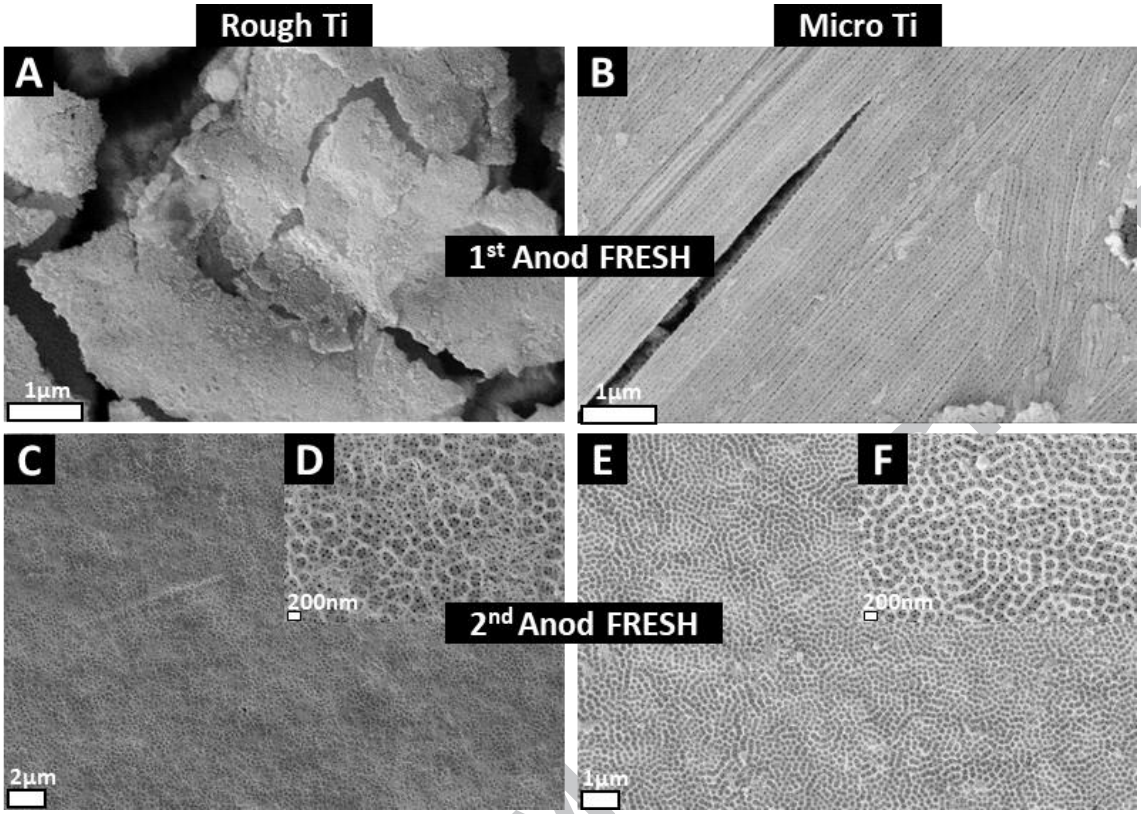

Fig. 3. SEM images for comparison of multi-step EA performed on Rough-Ti/Micro-Ti with fresh electrolyte. (A-B) 1st EA, 60V 10min, (C-F) 2nd EA, 60V 10min. 2nd EA was performed on the Rough/Micro templates after removal of the anodic film (fabricated by EA using fresh electrolyte at 75V 2h). EA: electrochemical anodization.

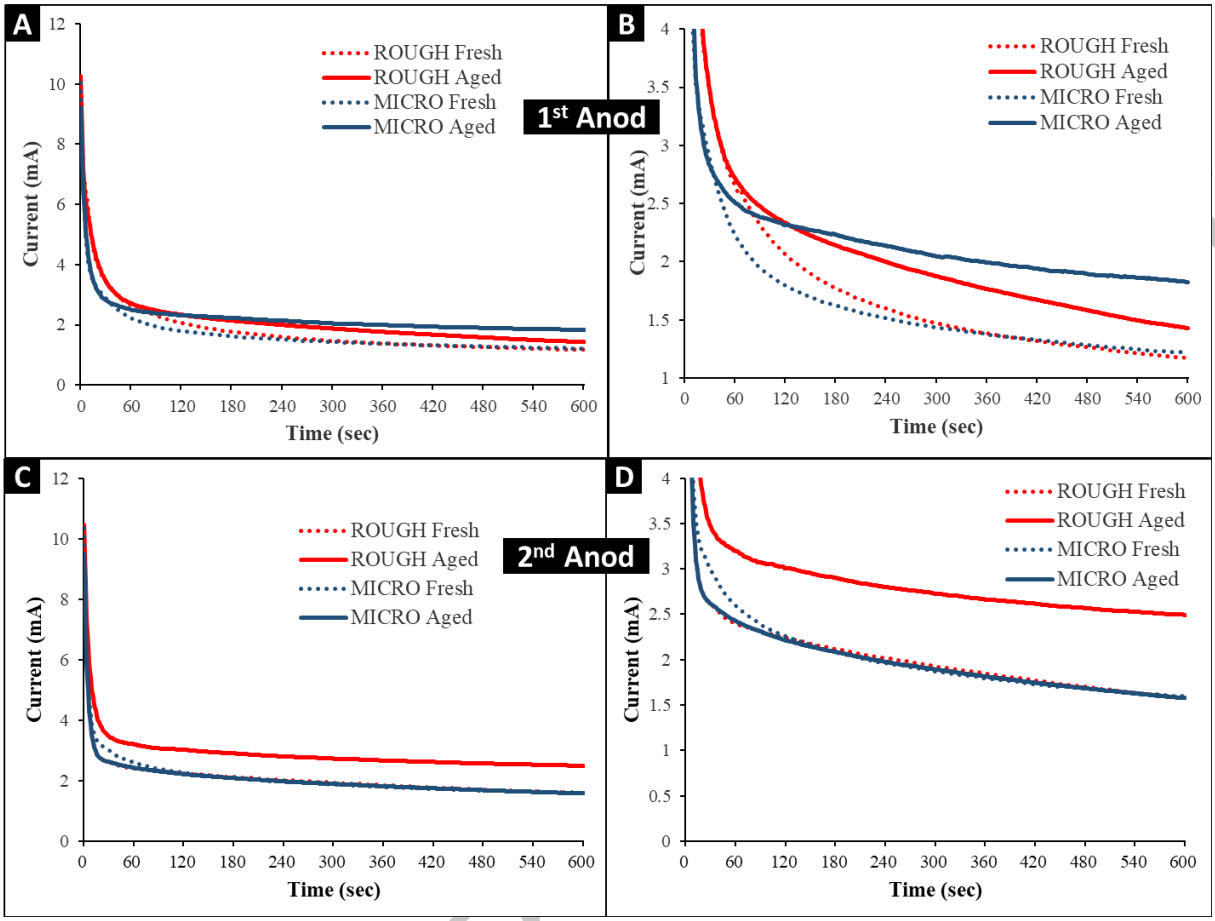

Fig. 4. Current vs time plots of EA performed on Rough-Ti/Micro-Ti with fresh and aged electrolyte systems. (A-B) 1st EA, 60V 10min, and (C-D) 2nd EA, 60V 10min. 2nd EA was performed on the Rough/Micro templates after removal of the anodic film (fabricated by EA using fresh electrolyte at 75V 2h). Anod: electrochemical anodization.

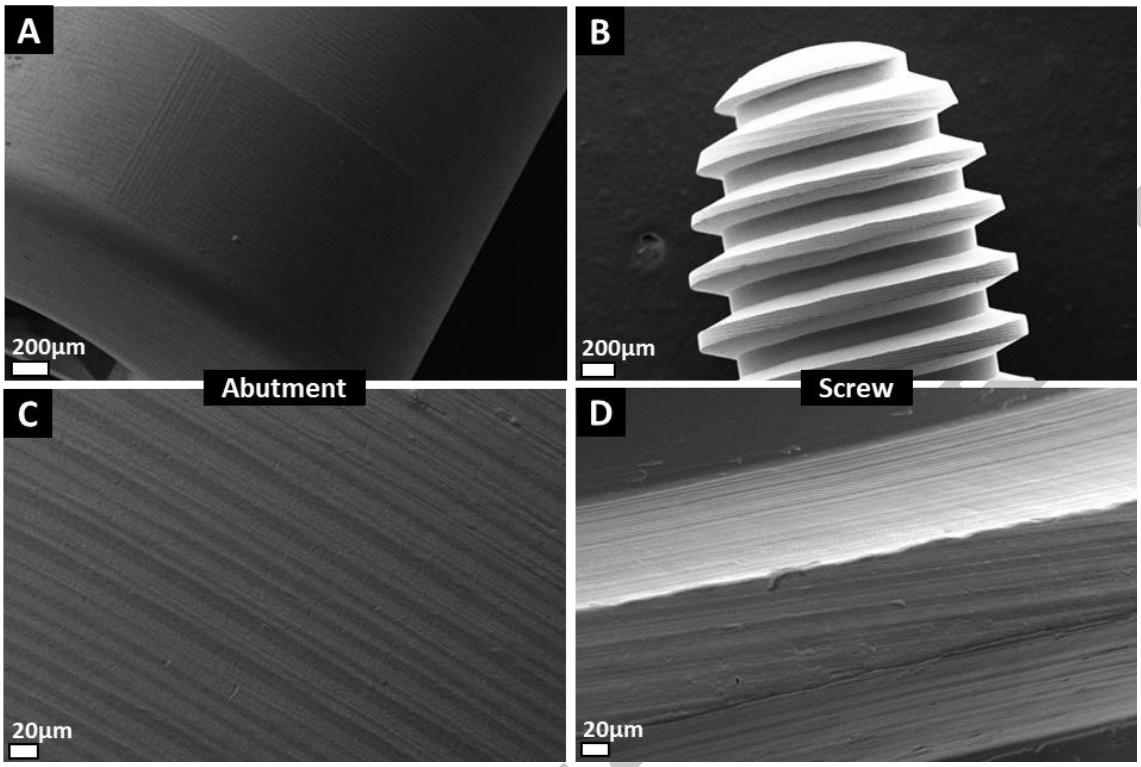

Fig. 5. SEM images of commercial titanium dental implants with micro-rough/machined surfaces: (A, C) cylindrical abutment, and (B, D) tapered screw.

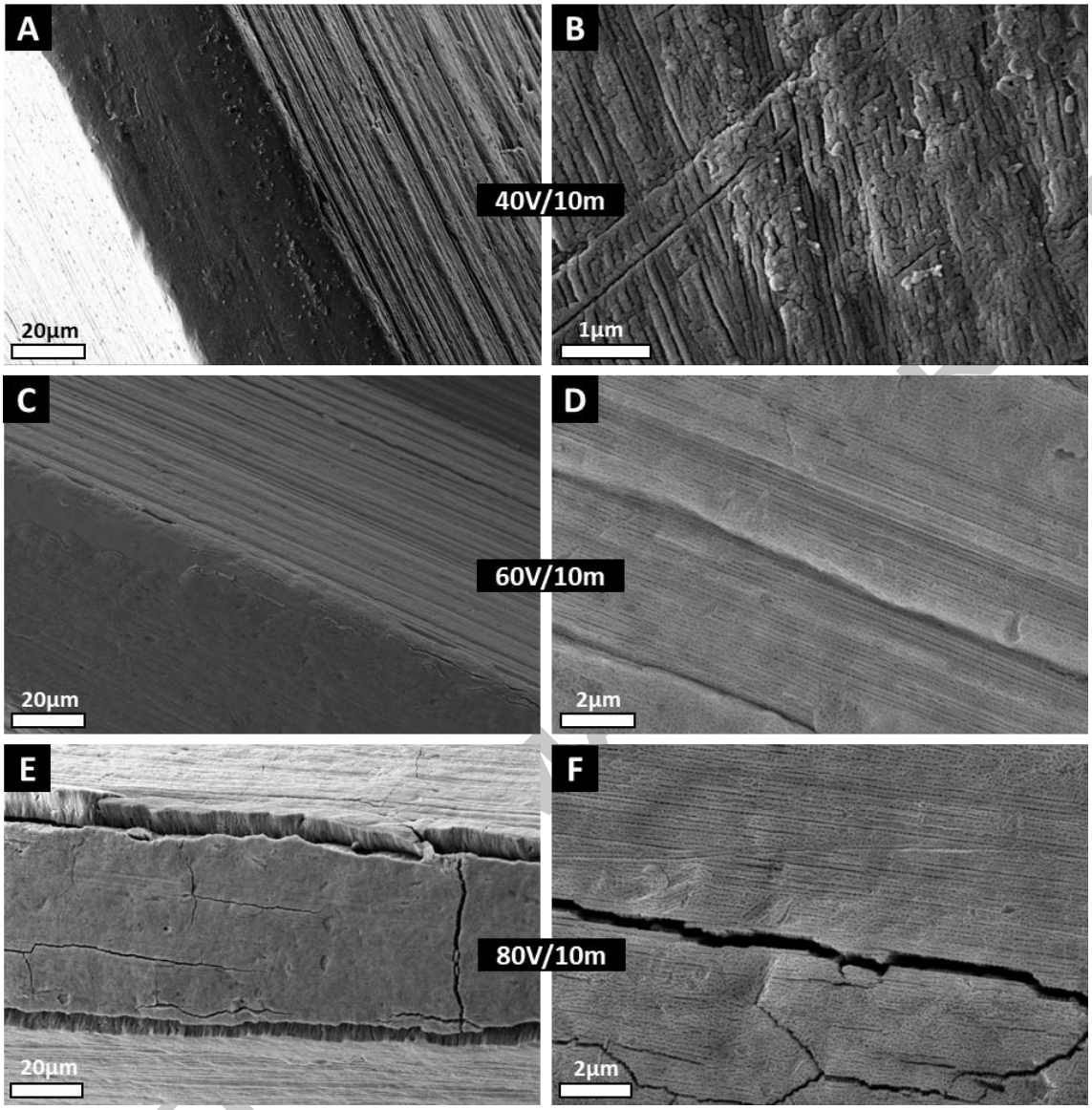

Fig. 6. Anodization optimization on Ti screws towards obtaining mechanically stable nanoporous coating. SEM images showing the close up of the screw-threads (sharp-edges, prone to fracture): (A-B) 40V 10 min, (C-D) 60V 10 min, and (E-F) 80V 10min.

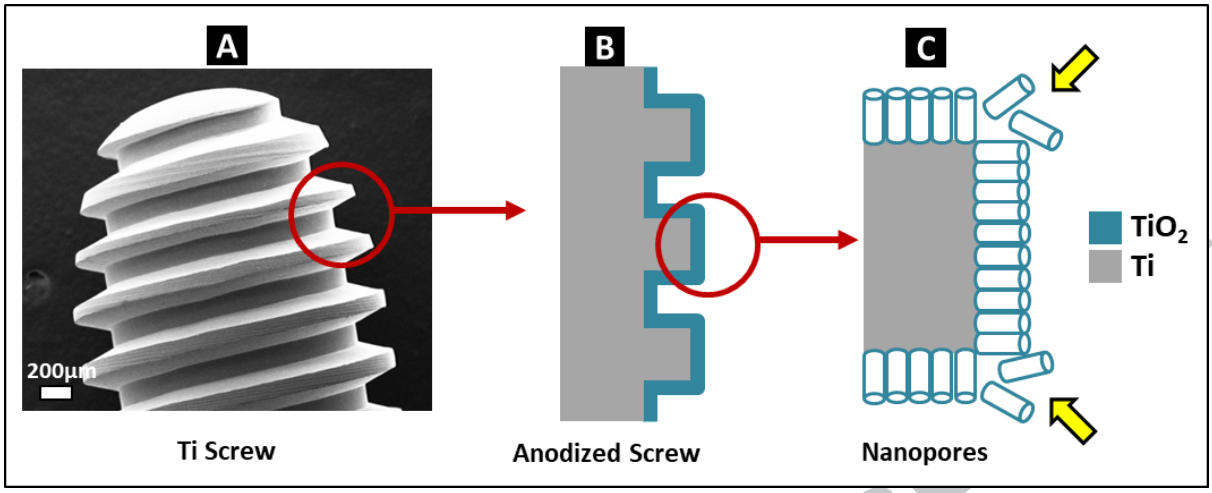

Fig. 7. Electrochemical anodization (EA) of titanium implant screws: (A) top-view SEM image showing threads of the implant screw, and (B-C) schematic representation of anodized screw with nanopores, highlighting the areas (yellow arrows) where stability of the anodic nanostructures may be compromised leading to delamination and fracture.

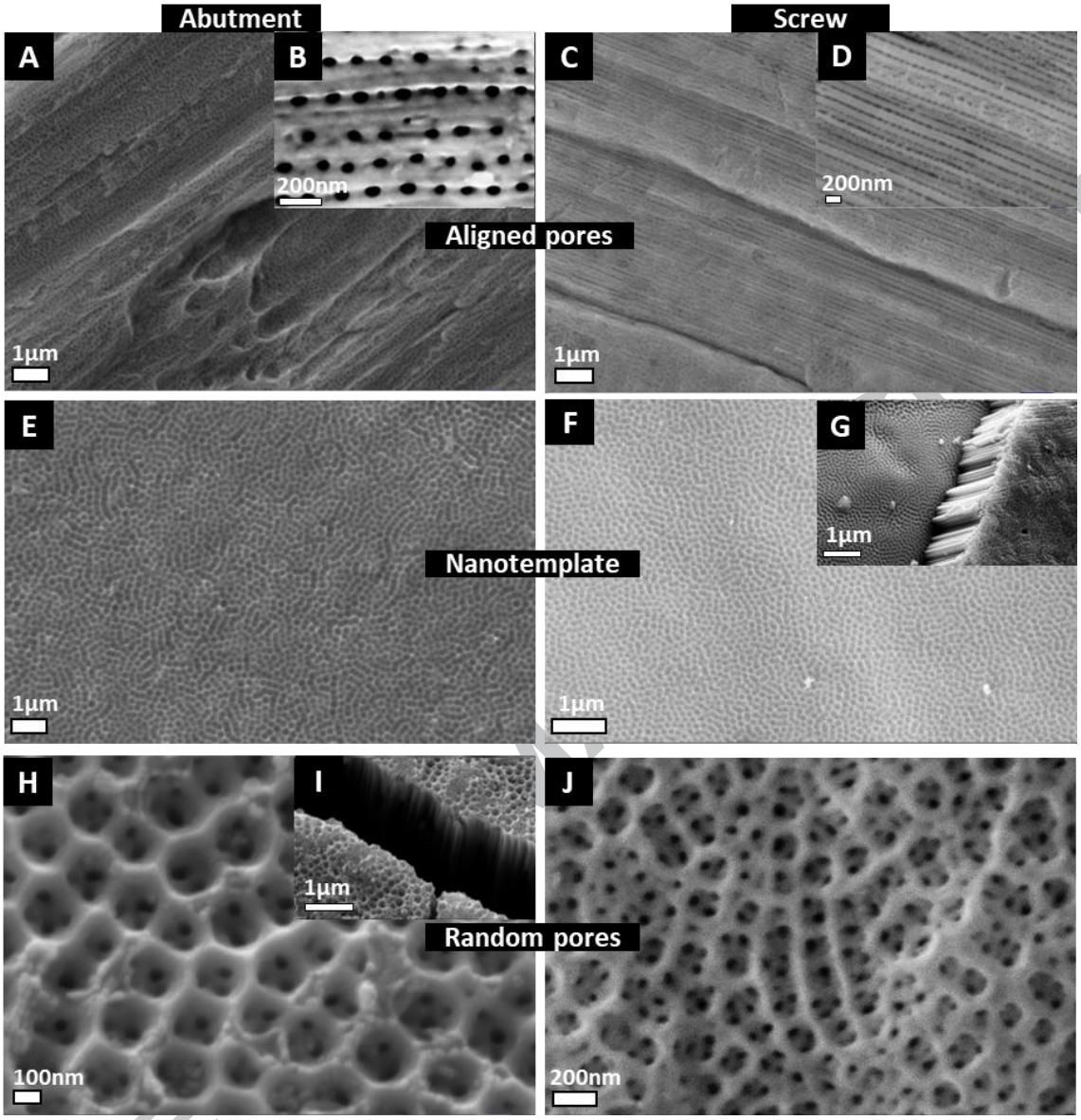

Fig. 8. Optimized nanotopographies applied onto commercial titanium implant surfaces: abutment and screw. SEM images showing: (A-D) 1st anodization at 60V 10m using aged electrolyte to preserve the underlying micro-features; (E-G) nanotemplated substrate achieved by removing the 1st anodized TNT film (fresh electrolyte, 75V 2h) [(G) partially fractured anodized surface showing nanotubes/pores with template surface]; and (H-J) 2nd anodization performed on nanotemplates to yield random nanopores (aged electrolyte, 60V 10 min).

Table 1. Variation of elastic modulus and hardness of titania nanopores fabricated on Ti wire (representative of dental abutment), anodized with aged or fresh electrolyte. The values are presented with increasing indentation depth using Berkovich indenter. The anodization was performed at 60V for 10min. *: $p<0.05$ compared with values from 50 nm within the same group.

Indentation Depth (nm)	**Elastic Modulus (GPa)**		**Hardness (GPa)**	
	Aged	Fresh	Aged	Fresh
50	63.18±2.4	39.42±4.6	2.76±1.1	0.95±0.4
100	63.90±5.7	38.49±2.5	2.20±0.6	0.51±0.1*
150	61.70±1.8	42.07±14.7	2.04±0.4	0.52±0.1*
200	58.30±5.2	45.83±8.7	1.94±0.4	0.53±0.1*
250	59.78±4.8	48.72±8.4	1.91±0.4	0.60±0.2
300	60.39±5.1	50.39±9.0	1.94±0.3	0.67±0.2

Grapphical abstract: